KI REPORTS
KIReports.org
TRANSLATIONAL RESEARCH

In Vivo Expression of NUP93 and Its Alteration by *NUP93* Mutations Causing Focal Segmental Glomerulosclerosis

Taeko Hashimoto[1,2,3], Yutaka Harita[3], Keiichi Takizawa[3], Seiya Urae[3], Kiyonobu Ishizuka[2], Kenichiro Miura[2], Shigeru Horita[2], Daisuke Ogino[1], Gen Tamiya[4,5], Hideki Ishida[6], Tetsuo Mitsui[1], Kiyoshi Hayasaka[1,7] and Motoshi Hattori[2]

[1]Department of Pediatrics, Yamagata University School of Medicine, Yamagata, Japan; [2]Department of Pediatric Nephrology, Tokyo Women's Medical University, School of Medicine, Tokyo, Japan; [3]Department of Pediatrics, Graduate School of Medicine, The University of Tokyo, Tokyo, Japan; [4]Tohoku Medical Megabank Organization, Tohoku University, Sendai, Japan; [5]RIKEN Center for Advanced Intelligence Project, Tokyo, Japan; [6]Department of Urology, Tokyo Women's Medical University, School of Medicine, Tokyo, Japan; and [7]Department of Pediatrics, Miyukikai Hospital, Kaminoyama, Japan

Introduction: Mutations in genes encoding nucleoporins (NUPs; components of nuclear pore complexes [NPCs]), such as *NUP93*, have been reported to cause steroid-resistant nephrotic syndrome (SRNS) or focal segmental glomerulosclerosis (FSGS), which often progresses to end-stage renal disease (ESRD) in childhood. The expression of NUP93 in renal or extrarenal tissues, and the mechanism by which *NUP93* mutations cause this renal phenotype, remain unclear.

Methods: The expression of NUP93 in normal control kidney and in a patient with FSGS carrying *NUP93* mutations was examined by immunofluorescence analysis. The expression of NUP93 in blood cells was analyzed by Western blot analysis.

Results: Immunofluorescence analysis detected NUP93 expression in nuclei of all glomerular and tubulointerstitial cells in human kidneys. Whole-exome sequencing identified a compound heterozygous *NUP93* mutation comprising a novel missense mutation p.Arg525Trp, and a previously reported mutation, p.Tyr629Cys, in a patient with FSGS that developed ESRD at the age of 6 years. In the patient's kidney, the intensity of NUP93 immunofluorescence was significantly decreased in the nuclei of both glomerular and extraglomerular cells. The expression of CD2-associated protein (CD2AP) and nephrin in the patient's podocytes was relatively intact. The amount of NUP93 protein was not significantly altered in the peripheral blood mononuclear cells of the patient.

Conclusion: NUP93 is expressed in the nuclei of all the cell types of the human kidney. Altered NUP93 expression in glomerular cells as well as extraglomerular cells by *NUP93* mutations may underlie the pathogenic mechanism of SRNS or FSGS.

Kidney Int Rep (2019) **4,** 1312–1322; https://doi.org/10.1016/j.ekir.2019.05.1157
KEYWORDS: focal segmental glomerulosclerosis; nuclear pore complex; nucleoporin; NUP93; steroid-resistant nephrotic syndrome

FSGS is a group of clinicopathological entities[1–3] involving the glomerulus. Clinically, FSGS exhibits a large overlap with the clinical features of SRNS in children and adults.[4,5] FSGS is classified into primary (idiopathic) and secondary forms.[6,7] Secondary FSGS occurs as an adaptive response to known causes, including genetic abnormalities.[7–9] Mutations in more than 50 genes have been associated with genetic FSGS.[10–12] A single mutation was identified in approximately 30% of a mostly pediatric SRNS cohort.[7,13,14]

NPCs form an octagonal channel across the nuclear envelope that mediate nucleocytoplasmic transport. They are some of the largest molecules found in cells.[15–17] NPCs have molecular masses of approximately 120 MDa in humans, and are built from multiple copies of different nuclear pore proteins called nucleoporins (NUPs).[15,16,18] Although NUPs are conserved across eukaryotes, and the overall structure of NPCs is conserved in all cell types, the protein composition of NPCs varies among cell or tissue types.[15,19–21] In addition to their role in nucleocytoplasmic transport, NPCs are also involved

Correspondence: Yutaka Harita, Department of Pediatrics, Graduate School of Medicine, The University of Tokyo, 7–3–1 Hongo, Bunkyo-ku, Tokyo 113–8655, Japan. E-mail: haritay-ped@h.u-tokyo.ac.jp

Received 17 March 2019; revised 14 May 2019; accepted 23 May 2019; published online 31 May 2019

in chromatin organization, which regulates gene expression and DNA repair.[15,19,22,23] Genetic alterations in NUP genes are linked to different cellular and developmental defects resulting in immune, cardiovascular, or neurological abnormalities.[17,24]

In 2016, homozygous mutations in *NUP93* (p.Gly591Val or p.Tyr629Cys) were identified in 3 familial SRNS cases.[25] In that study, the authors demonstrated that NUP93 is expressed in developing podocytes at the capillary loop stage in fetal rat kidney, and some truncating mutations resulted in a defect in its localization along the nuclear envelope in cultured podocytes. NUP93 and other NUP-associated molecules regulate the bone morphogenetic protein-7–dependent SMAD signaling pathway, and some of mutations in *NUP93,* including p.Lys442Asnfs*14, p.Gly591Val, and p.Tyr629Cys have been reported to abrogate the signal.[25]

So far, it has been unclear whether NUP93 is expressed only in specific cell types in the kidney, such as podocytes. It also has not yet been shown whether FSGS-causing *NUP93* mutations alter the expression or localization of NUP93 in podocytes as well as in other renal cells. Furthermore, its expression in extrarenal tissues or cells has been incompletely analyzed.[25]

In this study, we characterized NUP93 expression in human renal tissues. The expression of NUP93 in kidney and blood cells in a patient with FSGS carrying compound heterozygous *NUP93* mutations was also analyzed.

MATERIALS AND METHODS

Compliance With Ethical Standards

This study was approved by the ethics committee of Yamagata University (#2012–87). Informed consent was obtained from all participants included in this study.

Histological Analysis

Tissue for light microscopy was collected and processed routinely. Biopsy tissue was routinely fixed for electron microscopy. Immunohistological analysis of podocyte protein expression was performed as follows. Paraffin-embedded samples from human renal biopsy samples were deparaffinized in xylene and rehydrated through an ethanol-H_2O gradient, followed by incubation in a target retrieval solution (S1699; DAKO, Carpinteria, CA) for 20 minutes at 121 °C. Sections were cooled to room temperature and incubated with Alexa Fluor–conjugated secondary antibodies (Invitrogen, Carlsbad, CA). Images were obtained using fluorescence microscopy and a confocal microscope (model LSM-710; Carl Zeiss, Oberkochen, Germany) and were processed using commercial imaging software (Adobe Photoshop CC 2017; Adobe, Inc., San Jose, CA).

The following antibodies were obtained commercially: mouse monoclonal anti-NUP93 antibody raised against amino acids 1–300 mapping at the N-terminus of NUP93 of human origin (Santa Cruz Biotechnology, Inc., Santa Cruz, CA), rabbit polyclonal anti-CD2AP antibody (Sigma-Aldrich, St. Louis, MO), rabbit polyclonal anti-CD31 antibody (Spring Bioscience, Inc., Pleasanton, CA), and rabbit polyclonal anti-amnionless antibody (Sigma-Aldrich). Rabbit polyclonal anti-nephrin IgG has been described previously.[26] Control samples (donor kidney or biopsy samples from patients with nephrotic syndrome during a proteinuric period) were stained at the same time.

Expression Vectors

Full-length cDNA for human *NUP93* was amplified by polymerase chain reaction from cDNA derived from HEK293T cells, using the following primer sets: 5′-AAGAGCCCGGGCGGATCCATGGATACTGAGGGGTTT GGTGAGCTCCTT-3′ and 5′-CCCCCCCTCGAGGTC GACTTAATTCATGAGGACCTCCATCTGCACCAG-3′. After digestion of pCMV-tag2b vector with BamHI and SalI, *NUP93* cDNA was inserted (Gibson Assembly Master Mix; New England Biolabs, Ipswich, MA) according to the manufacturer's instructions. The product generated by polymerase chain reaction was confirmed by nucleotide sequencing.

Preabsorption of NUP93 Antibody

HEK293T cells were purchased from the American Type Culture Collection (Manassas, VA) and maintained in Dulbecco's modified Eagle's medium containing 10% fetal bovine serum. Transfections were performed using a polyethylene-imine reagent (PEI-Max; Polysciences, Warrington, PA) following the manufacturer's instructions. Cells were lysed in a buffer (20 mM Tris–HCl [pH 7.5], 150 mM NaCl, 1 mM EDTA, and 1% NP-40) containing a protease inhibitor cocktail (Nacalai Tesque, Kyoto, Japan) for 10 minutes on ice. Lysates were clarified by centrifugation. Of the lysates, 2% were used for sodium dodecyl sulfate–polyacrylamide gel electrophoresis and immunoblotting; the rest of the lysates were incubated with agarose beads conjugated with anti-FLAG peptide M2 antibody for 1 hour at 4 °C. The diluted primary antibody for NUP93 was incubated with the immunoprecipitates from cells transfected with FLAG-NUP93 or control vector (FLAG-LAMB2) for antibody absorption.

Peripheral Blood Mononuclear Cell Collection and Quantification of the NUP93

Blood samples were collected in EDTA-treated tubes and peripheral blood mononuclear cells (PBMCs) were

isolated by density gradient centrifugation (Lymphocyte Separation Solution: d = 1.077 g/ml; Nacalai Tesque). PBMCs were washed once in RPMI 1640 medium and the cell suspensions were centrifuged at 300G for 2 minutes. The supernatant was discarded and lysis buffer added, followed by incubation on ice for 10 min. After centrifugation at 20,000G for 15 minutes, the pellets were solubilized in sodium dodecyl sulfate sample buffer and sonicated for 1 minute, then incubated at 95 °C for 5 minutes. The lysates were used for sodium dodecyl sulfate–polyacrylamide gel electrophoresis and Western blot analysis.

Whole-Exome Analysis and *NUP93* Gene Analysis

Whole-exome analysis was performed using a previously described method.[27] Briefly, genomic DNA was extracted from peripheral blood. Exon capture was performed with a commercial kit (SureSelect Human All Exon kit v5; Agilent Technologies, Santa Clara, CA). Exon libraries were sequenced (HiSeq 2000 platform; Illumina, San Diego CA) according to the manufacturer's instructions. Paired 100-base pair reads were aligned to the reference human genome (UCSC hg19) using the Burrows-Wheeler Aligner (Version 0.7.3a).[28] Single-nucleotide variants and indels were identified as previously described.[29] We focused on the variants of 53 FSGS/SRNS causative genes (Supplementary Table S1). Then, variant filtering on the basis of population frequency was performed to include only minor allele frequencies of <1% of healthy control population databases.[30,31] Variants that were protein-truncating, highly conserved across species, predicted to be deleterious based on at least 2 of 3 programs' prediction scores from the web-based prediction programs PolyPhen-2 (http://genetics.bwh.harvard. edu/pph2), SIFT (Sorting Intolerant From Tolerant) (http://sift.bii.a-star.edu.sg/), and MutationTaster (http://www.mutationtaster.org), were left. At this point, 5 variants remained. Three of them were excluded because they were reported as heterozygotes, whereas their genetic forms were autosomal recessive. Eventually, the 2 variants of *NUP93* (c.1573C>T and c.1886A>G) remained. Sanger sequencing was performed to detect *NUP93* and validate the presence of each variant detected by exome sequencing in the patient and her parents and brother. The entire cording region and exon-intron boundaries of all cording exons of *NUP93* gene were amplified from the genomic DNA using polymerase chain reaction. The sequence reactions were analyzed on an ABI PRISM 3100 Genetic Analyzer (PE Applied Biosystems, Foster City, CA) with the BigDye Terminator

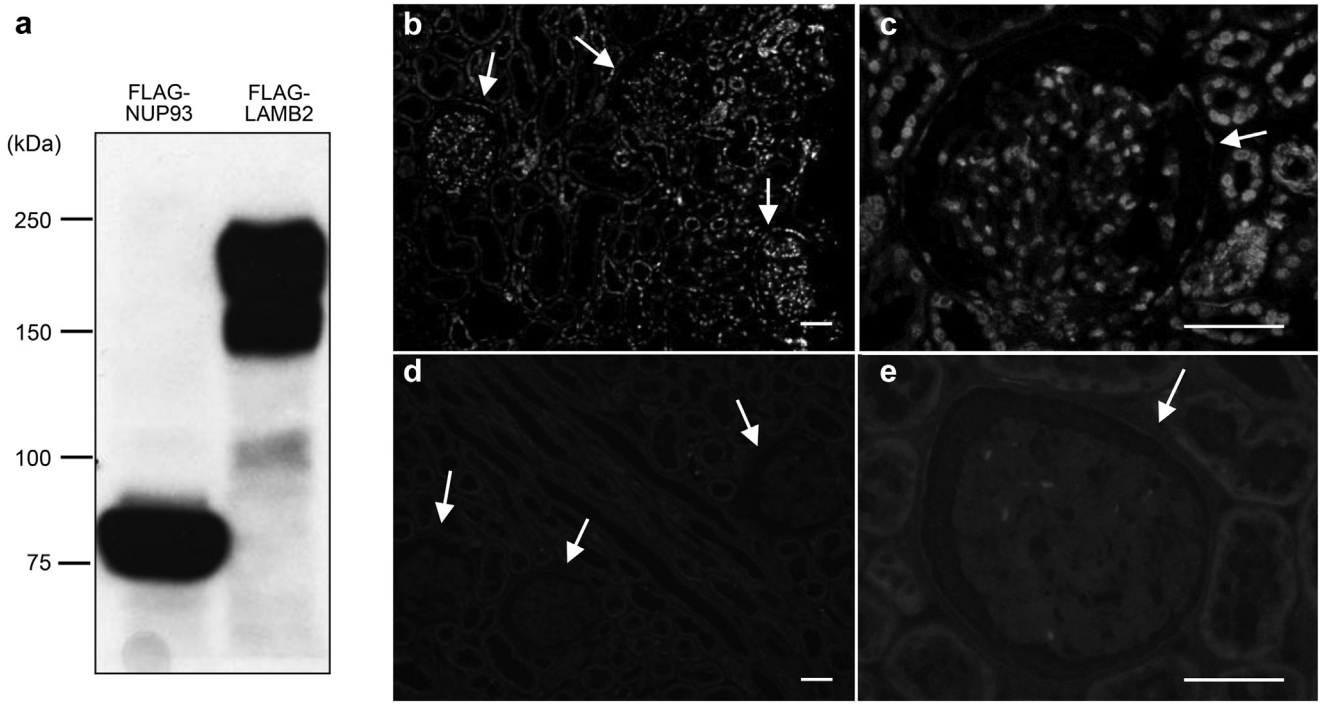

Figure 1. Nucleoporin (NUP)93 expression in the human kidney cortex. Lysates of HEK293T cells transiently expressing FLAG-NUP93 or FLAG-laminin β2 (LAMB2) were immunoprecipitated with anti-FLAG antibody and analyzed by Western blot with the indicated antibodies (a). These immunoprecipitates were used for antibody absorption. Human kidney sections were stained with anti-NUP93 antibody preabsorbed with anti-FLAG immunoprecipitates from lysates of HEK293T cells that expressed control (flag-LAMB2) vector or flag-tagged NUP93 (b–e). The NUP93 signals were detected in cells both inside and outside of glomeruli of control kidneys with the preincubated lysate of the control vector (b,c). No staining was detected with anti-NUP93 antibody preabsorbed immunoprecipitates from lysates of flag-tagged NUP93 vector (d,e). Glomeruli are indicated by arrows. Bar = 50 μm.

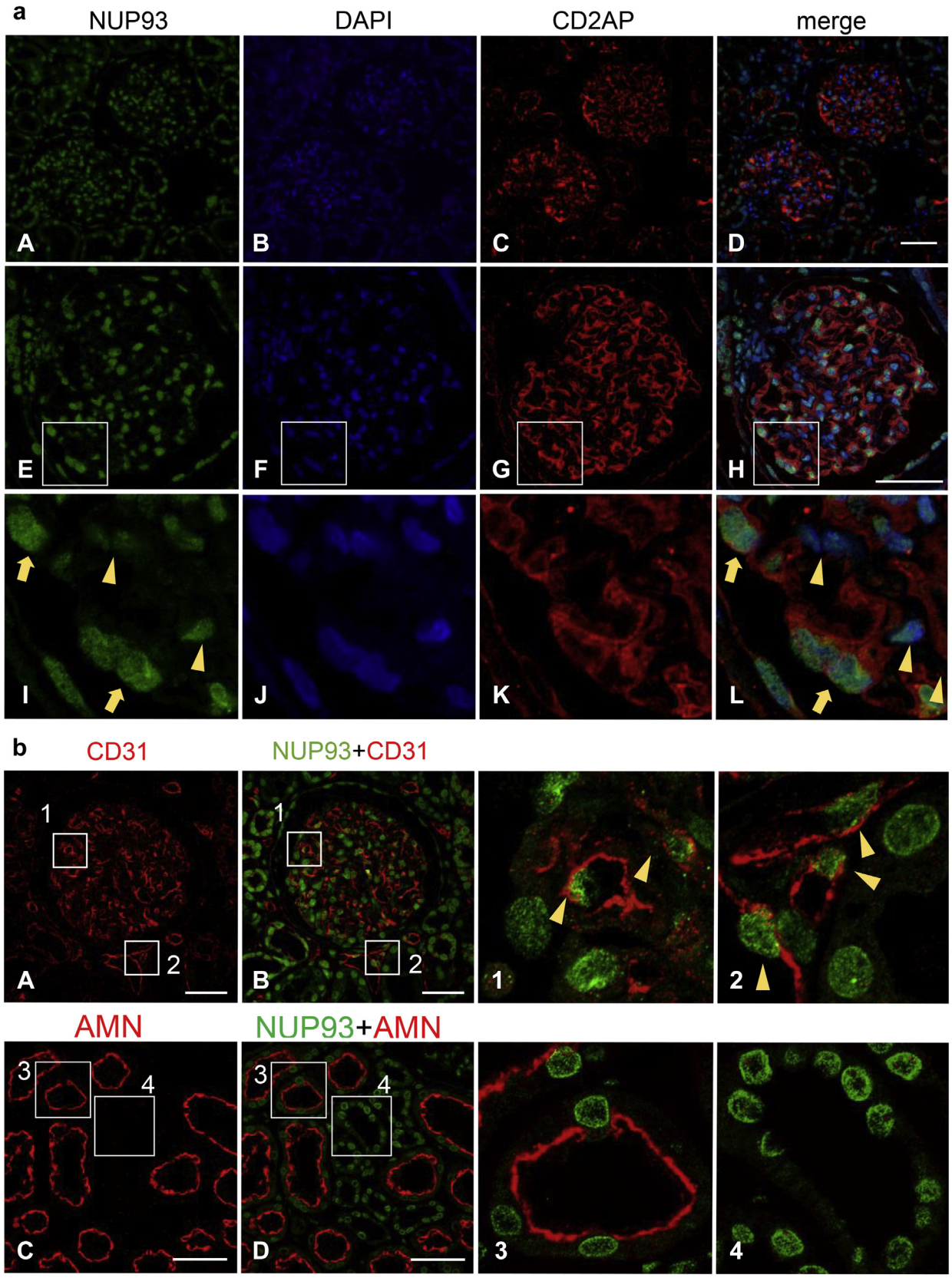

Figure 2. Nucleoporin (NUP)93 expression and localization in the human kidney cortex. (a) Human kidney sections were stained with anti-NUP93 antibody (green), anti– CD2-associated protein (CD2AP) antibody (red), and 4′,6-diamidino-2-phenylindole (DAPI) (blue). Top row: Low magnification images of the human kidney cortex (A–D). Middle row: High-magnification images of the human kidney cortex by confocal microscopy (E–H). Bottom row: The enlarged view of the white square frame of the images (I–L). Staining for NUP93 was detected in glomerular cells as well as in cells outside of glomeruli, such as tubulointerstitial cells (A–D). Staining for NUP93 was detected in the nucleus of the cells not only inside of (continued)

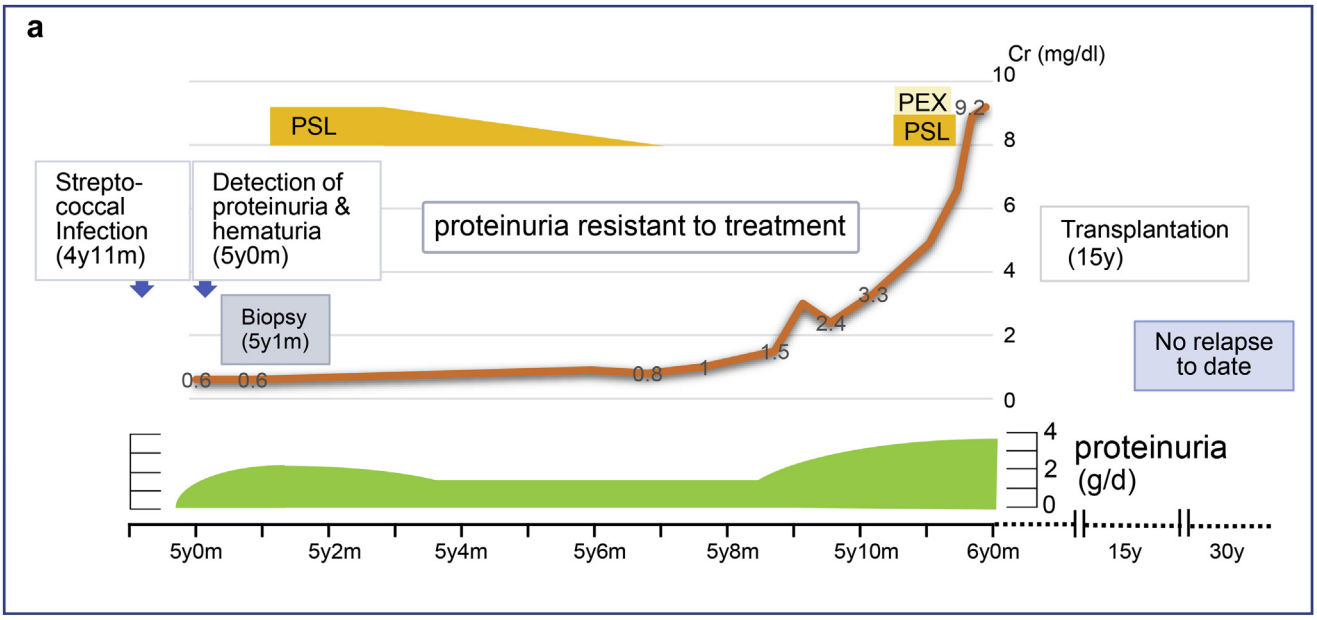

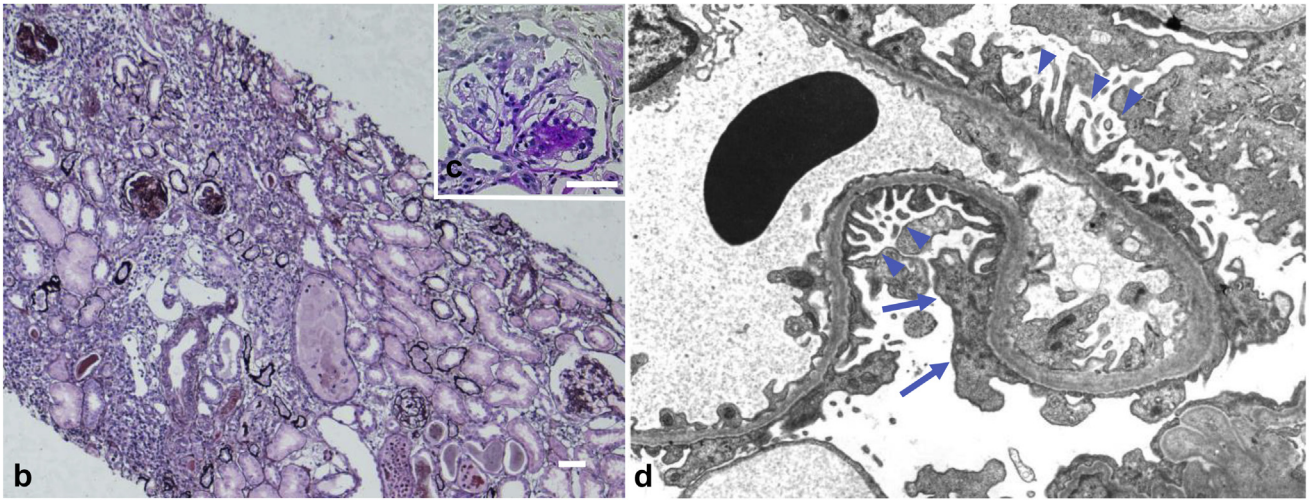

Figure 3. Clinical course and kidney histology of the affected individual with *NUP93* mutations. Clinical course of the patient with focal segmental glomerulosclerosis carrying *NUP93* mutations (a). Light microscopy of kidney tissue from the patient (b: periodic acid-methenamine silver stain, original magnification ×100; c: periodic acid–Schiff stain, original magnification ×400). Electron microscopy of glomerular capillary of the patient (d). Severe atrophy of tubuloepithelial cells, interstitial fibrosis, and infiltration of inflammatory cells was observed (b). The biopsy specimen included 21 glomeruli, 18 of which showed global sclerosis and 1 of which showed segmental sclerosis (c). Podocytes (arrowheads) with only focal effacement (arrows) were observed (magnification unknown; d). PEX, plasma exchange; PSL, prednisolone. Bar = 50 μm.

Cycle Sequencing Ready Reaction Kit (PE Applied Biosystems).

RESULTS

Expression of NUP93 in the Human Kidney

NUP93 expression in human kidney samples was analyzed by using monoclonal antibodies raised against the 300 N-terminal amino acids of human NUP93. This antibody specifically recognizes NUP93 expressed in HEK293 cells (Figure 1a). In control kidneys, the immunofluorescent signals for NUP93 were detected in cells both inside and outside of glomeruli (Figure 1b and c). The signals for NUP93 were significantly decreased when antibody was preabsorbed with anti-FLAG

Figure 2. (continued) glomeruli but also in parietal glomerular epithelial cells in the control specimen (E–H). In glomeruli, NUP93 was detected in the nucleus of podocytes (I–L, yellow arrows) and the other cells of glomeruli (yellow arrowheads). (b) Double-staining of human kidney cortex with anti-NUP93 antibody (green) and anti-CD31 antibody (red) (A,B) or anti-amnionless (AMN) antibody (red) (C,D), and the enlarged view of the white square frames of the images (1–4). Upper row: NUP93 in endothelial cells. NUP93 was detected on nuclei of both glomerular endothelial cells (A, B, and 1, arrowheads) and endothelial cells outside of glomeruli (A, B, and 2, arrowheads). Lower row: NUP93 in tubulointerstitial cells. NUP93 was detected in nuclei of both proximal tubular cells (AMN-positive cells) (C, D, and 3) and in AMN-negative cells (C, D, and 4). Bar = 50 μm.

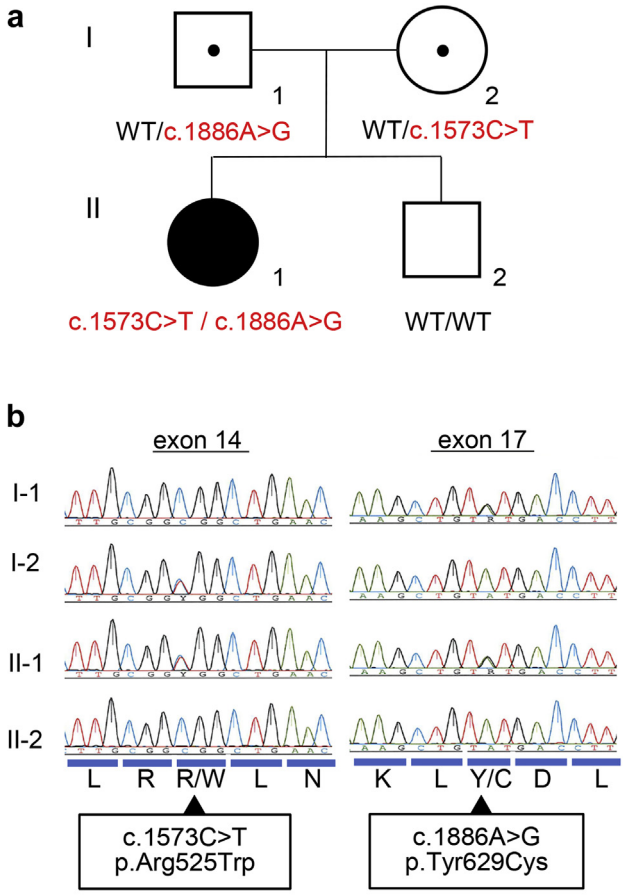

Figure 4. Identification of a novel compound heterozygous mutation of *NUP93*. Patient's pedigree. Red = Mutant alleles, WT = wild-type allele (a). Sequence chromatograms for exon 14 and exon 17 of *NUP93* for the patient and her family (b). Protein alignment plot of the nucleoporin (NUP)93 amino acid (AA) sequence for residues 518–532 in exon 14 and 622–636 in exon 17 of NUP93 (c). R, Arg; L, Leu; R/W, Arg/Trp; N, Asn; K, Lys; Y/C, Tyr/Cys; D, Asp.

immunoprecipitates from cell lysates of HEK293 cells that express FLAG-tagged NUP93 (Figure 1d and e), indicating the specificity of the signals.

To determine the localization of NUP93 in glomeruli, the human kidney sections were double-labeled with NUP93 and CD2AP (Figure 2a). CD2AP is expressed in podocytes in glomeruli.[32] The signals for NUP93 were detected both in the glomerular cells and in tubulointerstitial cells around glomeruli (Figure 2a, A–D). NUP93 signals were detected in all nuclei in the glomerular cells as well as those in parietal glomerular epithelial cells (Figure 2a, E–H). The signals for NUP93 in glomeruli were also observed in cells expressing CD2AP (podocytes) (Figure 2a, I–L, yellow arrows), as well as in CD2AP-negative cells (Figure 2a, I–L, yellow arrowheads).

To confirm the expression of NUP93 in endothelial cells, double-staining with CD31, an endothelial marker, was performed, and revealed expression of NUP93 in endothelial cells both within and outside the glomeruli (Figure 2b, A, B, 1, and 2). For the renal tubules, we performed double-staining with NUP93 and amnionless, as a marker of proximal tubules,[33] and confirmed that NUP93 was expressed in the form of dots in the nuclei of the proximal tubules (Figure 2b, C, D, and 3)and distal tubules (Figure 2b, C, D, and 4) of the human kidney sections.

To confirm whether NUP93 is ubiquitously expressed in kidney cells, NUP93-positive cells and cells positive for 4′,6-diamidino-2-phenylindole were quantitated using high-magnification images of 5 different glomeruli and those of the tubulointerstitial cells in the human kidney cortex. More than 99% of cells positive for 4′,6-diamidino-2-phenylindole in the samples were NUP93-positive both in glomeruli and in extraglomerular cells, indicating that NUP93 is expressed throughout the human renal cortex.

Patient With FSGS With Mutations of *NUP93*

We identified a compound heterozygous mutation of *NUP93* in young Japanese woman with FSGS. In this patient, microscopic hematuria, proteinuria, and hypertension were first detected after streptococcal infection at the age of 4 years and 11 months. Her paternal grandfather and maternal grandfather had died of cancer, but she had no family history of kidney disease. She had a history of an afebrile convulsion at the age of 5 years, and febrile seizures at the ages of 9 and 11 years. She developed rheumatoid arthritis at the age of 17 years.

Because of persistent proteinuria (2–2.5 g/d) and hypoalbuminemia (2.8 g/dl), renal biopsy was performed at the age of 5 years and 1 month (Figure 3a). Light microscopy revealed that in a total of 21 glomeruli, global sclerosis was evident in 18 and segmental sclerosis was observed in 1. Mild tubular dilation with casts, as well as severe tubular interstitial infiltration and fibrosis were also observed (Figure 3b and c). Despite the diffuse and global glomerulosclerosis, electron microscopy revealed that the structure of the podocyte foot processes was largely maintained in the remaining glomeruli (Figure 3d). Positive staining for IgG (+) and C3 (+) in glomeruli were observed by immunofluorescence. From these histopathological results, she was diagnosed with FSGS.

Table 1. *NUP93* mutations in this case

Mutation	AA change	PolyPhen-2	Mutation taster	SIFT	1000G	gnomAD	EVS	HGVD	iJGVD
c.1573C>T	p.Arg525Trp	0.999[a]	0.999[a]	0.02[a]	0[b]	0.000004074[b]	0[b]	0[b]	0[b]
c.1886A>G	p.Tyr629Cys	1.0[a]	0.999[a]	0.06[a]	0[b]	0.000008133[b]	0[b]	0[b]	0[b]

AA, amino acid; EVS, NHLBI Exome Sequencing Project Exome Variant Server; gnomAD, The Gnome Aggregation Database; HGVD, Human Genetic Variation Database (the public exome database of the Japanese population); iJGVD, integrative Japanese Genome Variation Database[34]; SIFT, Sorting Intolerant From Tolerant; 1000G, 1000 Genomes Project data.
[a]Score of the variant in each web-based program.
[b]Frequency of the variant in each database.
Mutations are annotated according to NUP93 cDNA (GeneBank: NM_014669.4).

Proteinuria (1.5 g/d) did not respond to high-dose steroid therapy and her renal function progressively deteriorated. She had mild edema, which was easily controlled by diuretic agents. Plasma exchange was also performed but did not have any effect on proteinuria. She developed ESRD at the age of 6 years and was on chronic peritoneal dialysis. She received a living donor kidney transplant from her mother at 15 years. She is now 31 years old and has been hospitalized twice for suspected urinary tract infections at 28 and 30 years. Otherwise, she has been generally healthy and has suffered from no relapse of proteinuria or rejection after transplantation.

In this patient, 2 heterozygous mutations of *NUP93* were found in exons 14 and 17 (Figure 4) by whole-exome analysis. Direct sequencing confirmed that the patient had a compound heterozygous mutation in *NUP93*: c.1573C>T (predicting p.Arg525Trp) was

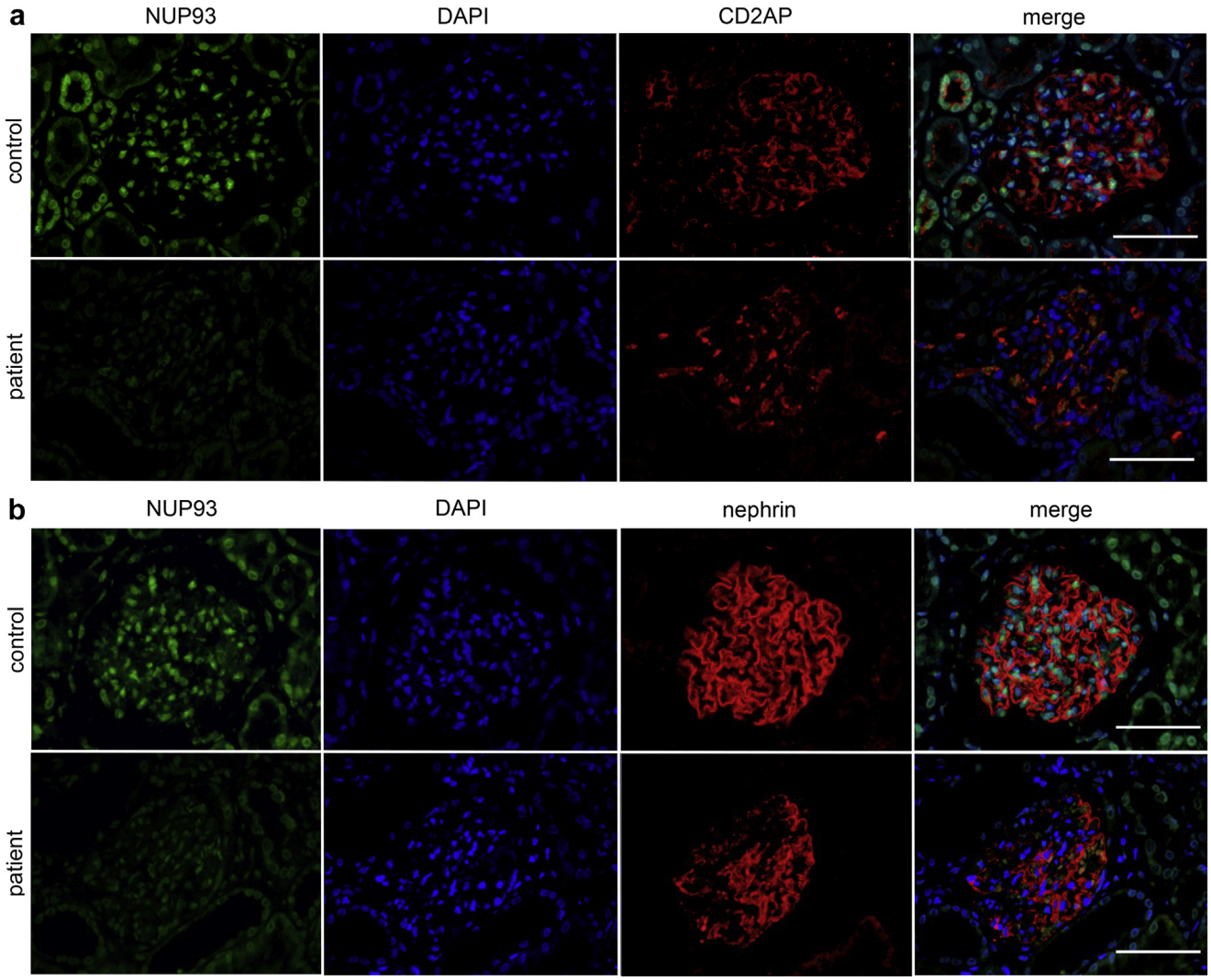

Figure 5. Expression of nucleoporin (NUP)93 in the patient with *NUP93* mutations. Dual-labeling immunofluorescence of NUP93 (green) with CD2-associated protein (CD2AP) (red; a) and NUP93 (green) with nephrin (red; b). The NUP93 signal was decreased in the whole biopsy specimen. The expression of CD2AP was maintained (a) and that of nephrin was only partially decreased (b) in the patient's glomeruli. Bar = 50 μm. DAPI, 4′,6-diamidino-2-phenylindole.

inherited from her healthy mother, and c.1886A>G (predicting p.Tyr629Cys) from her healthy father (Figure 4a and b). Tyrosine 629 of NUP93 is highly conserved between species and p.Tyr629Cys (rs757674160) was previously reported as a pathogenic Turkish founder allele.[25] The other variant in this case, p.Arg525Trp (rs760057496) was novel and also highly conserved between species (Figure 4c). Although these mutations had been registered in the database of single-nucleotide polymorphisms of the National Center for Biotechnology Information (dbSNP, www.ncbi.nlm.gov) and in the Genome Aggregation Database (gnomAD, http://gnomad.broadinstitute.org/; Supplementary Table S2),[31] the allele frequency was extremely low and homozygosity had not been reported (Table 1[34]). The functionality of p.Arg525Trp was analyzed using the SIFT web-based tool, PolyPhen2, and Mutation Taster by homology modeling and threading. All 3 models predicted NUP93 p.Arg525Trp to be pathogenic (Table 1).

Expression of NUP93 in the Patient With *NUP93* Mutation

We analyzed the expression of NUP93 in biopsy samples from the patient (Figure 5) by dual immunofluorescence assays with CD2AP (Figure 5a) or with nephrin (Figure 5b). In the patient's kidney, the staining intensity of NUP93 was diffusely decreased compared with control (donor kidney). The decrease of nuclear NUP93 signals was observed not only in glomerular cells but also in tubulointerstitial cells. Notably, glomerular expression of CD2AP was not significantly altered (Figure 5a) and nephrin was partially decreased only in sclerotic lesions of glomeruli (Figure 5b).

The expression of NUP93 in the patient's PBMCs was also examined by Western blot analysis. The specificity of the signal was confirmed by antigen preabsorption (Figure 6a). The amount of NUP93 protein in the patient's PBMCs did not significantly differ from those of control samples (Figure 6b).

To examine if the change in the renal expression of NUP93 in the patient was secondary to podocyte damage or proteinuria, the renal expression of NUP93 in patients with primary FSGS or with minimal change nephrotic syndrome was also analyzed. The staining pattern of NUP93 in a patient with minimal change nephrotic syndrome during a proteinuric state did not significantly differ from that in a control. In a patient with primary FSGS, the expression of NUP93 was also relatively maintained both in glomeruli and in renal tubules (Supplementary Figure S1). These results suggest that decreased signals of NUP93 in the patient with *NUP93* mutations may not be secondary to podocyte damage or proteinuria.

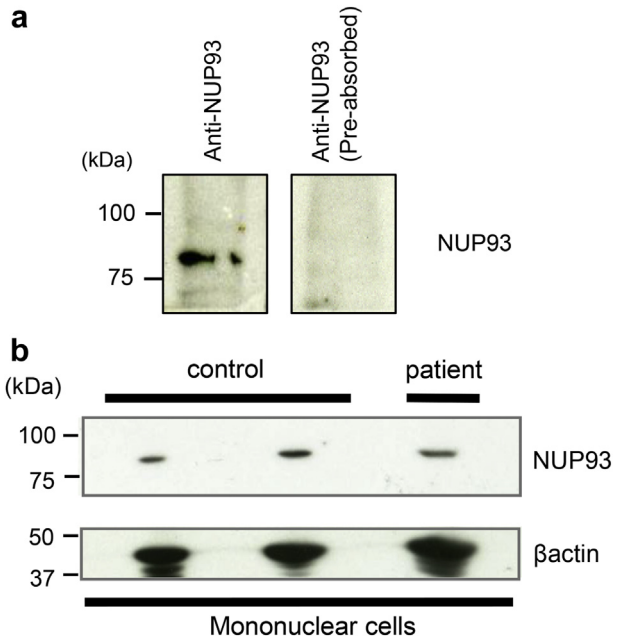

Figure 6. The expression of nucleoporin (NUP)93 in human peripheral blood mononuclear cells (PBMCs). Western blot analysis of NUP93 expression in human PBMCs (a). NUP93 was detected in the lysate from PBMCs from control samples. No staining was detected with anti-NUP93 antibody preabsorbed immunoprecipitates from lysates of flag-tagged NUP93. The amount of NUP93 in the patient's PBMCs analyzed by Western blot analysis (b). There was no noticeable change in the expression of NUP93 in the patient's PBMCs.

DISCUSSION

In this study, we identified a Japanese patient with FSGS with a compound heterozygous *NUP93* mutation. One of the mutations (p.Tyr629Cys) was the same variant as previously reported in patients with FSGS,[25] and the other variant, p.Arg525Trp, was novel. Because of the extremely low allele frequency and *in silico* prediction, this compound heterozygous mutation was predicted to be pathogenic. The 3-dimensional structure of human NUP93 created by SWISS-MODEL (http://swissmodel.expasy.org)[35,36] (Figure 7a) and all the mutations reported in previous studies[12,25,37] are shown in Figure 7b. The previous reports showed the onset of nephrotic syndrome or proteinuria between 1 and 7 years, and more than half of patients had hematuria and all patients developed ESRD between 1 and 12 years. The clinical features of the present case, who developed ESRD at 6 years, were consistent with these reports.[12,25,37] This is the first report of an East Asian patient with SRNS with the *NUP93* mutation.

We demonstrated that NUP93 expression is not confined to podocytes, but NUP93 is expressed in

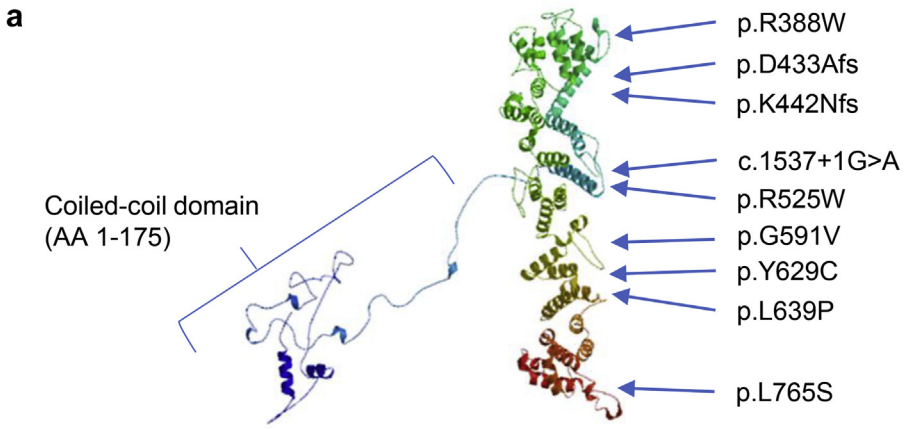

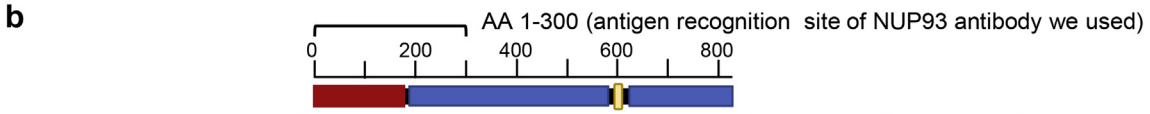

Variants of *NUP93*	Schematic position of each of the variants	Onset (Y)	ESRD (Y)	Ethnic origin	Ref.
c.1162C>T, p.R388W/ c.1772G>T, p.G591V		6	6	Serbian	[25]
c.1298delA, p.D433Afs/ c.1772G>T, p.G591V		3	3.5	CZSK	[37]
c.1326delG, p.K442Nfs c.1772G>T, p.G591V		~3	3	German	[25]
c.1537+1G>A, del ex13/ c.1772G>T, p.G591V		3 3	4 3	German CZSK	[25] [37]
c.1772G>T, p.G591V/ c.1772G>T, p.G591V		3 7	11 (CKD3)	Turkish CZSK	[25] [37]
c.1772G>T, p.G591V/ c.1916T>C, p.L639P		1.8	2.9	CZSK	[37]
c.1886A>G, p.Y629C/ c.1886A>G, p.Y629C		1 1	1 no data	Turkish Turkish	[25] [25]
c.2084T>C, p.L695S/ c.2267T>C, p.L756S		6.12	12	(White)	[12]
c.1573C>T, p.R525W/ c.1886A>G, p.Y629C		4	6	Japanese	*

Figure 7. Variants of *NUP93* reported in patients with focal segmental glomerulosclerosis (FSGS). Three-dimensional structure of human nucleoporin (NUP)93 created by the SWISS-MODEL[36] and a variant in FSGS. The template of this model was from PDB 5IJN[18] (a). Protein domain structure of human NUP93[25] and a schematic representation of *NUP93* mutation positions (b). The N-terminal coiled-coil region is marked in red; the alpha-helical regions are marked in blue. *NUP93* variants, age of onset and end-stage renal disease (ESRD), and ethnic origin of the present and previously reported patients are shown. The positions of variants are shown as colored squares. The European founder mutation (G591V), the Turkish founder mutation (Y629C),[25] and the other mutations are shown as orange, green, and gray squares, respectively. CKD3, chronic kidney disease stage 3; CZSK, Czech and Slovak; Ref, reference; Y, years. The asterisk refers to the present case.

several different cell types in the human kidney. In the patient carrying *NUP93* mutation, signal intensity for NUP93 was decreased in non–cell-type-specific fashion in renal cortex. In a previous report analyzing renal histology of patients with *NUP93* mutation, the authors found proximal tubular dilation with protein casts and interstitial cell infiltrations in some patients.[25] In the present case, severe atrophy of tubuloepithelial cells, interstitial fibrosis, and infiltration of inflammatory cells were evident in the biopsy specimen, although she had relatively mild proteinuria (2–2.5 g/d) and biopsy was done only a month after onset. Therefore, it may be possible that the alteration of NUP93 expression in extraglomerular cells is directly associated with tubulointerstitial lesions in the patient's kidney, whereas the possibility of tubulointerstitial damage secondary to glomerular sclerosis still cannot be dismissed.

The signals for NUP93 were significantly decreased in the cells in nonsclerotic regions in the patient's glomeruli, where CD2AP or nephrin expression was maintained. Sustained NUP93 expression in other patients with idiopathic nephrotic syndrome (Supplementary Figure S1) indicates a specific alteration of NUP93 expression in the patient carrying NUP93 mutations. When expressed in cultured podocytes, the *NUP93* Tyr629Cys mutation did not affect its expression level or its localization in nuclear pores despite its significantly decreased SMAD signaling.[25] The discrepancy with the *in vivo* expression in the patient's kidney might be because of the other variant p.Arg525Trp, or because of the difference between cells cultured *in vitro* and those *in vivo*.

In a previous report, knockdown of *NUP93* resulted in impaired migration and proliferation in immortalized human podocytes.[25] The depletion of NUP93 in *Caenorhabditis elegans* induced abnormal NPC distribution in the nuclear envelope and it caused a failure in nuclear exclusion of macromolecules,[38] which is crucial for cell viability. In the experiments using *Xenopus* spp., knockdown of *NUP93* led to a loss of cilia during embryonic development,[39] suggesting that function of *NUP93* can be context-dependent. Its altered expression in renal cells by the mutations of *NUP93* may lead to the altered viability of podocytes, which underlies the development of FSGS.

Further analysis of the role of the expression of NUP93 in renal and nonrenal cell types might reveal possible diverse effects on the affected patients.

DISCLOSURE

All the authors declared no competing interests.

ACKNOWLEDGMENTS

We thank Ms. Yumiko Kishikawa for her technical assistance. We thank Libby Cone, MD, MA, from Edanz Group (www.edanzediting.com/ac) for editing drafts of this manuscript.

This work was supported by Grants-in-Aid for Scientific Research (C) (subject ID: 18K07857 to MH and 18K07029 to YH, KI, and MH, and 16K10057 to TH and KH) from the Ministry of Education, Culture, Sports, Science and Technology of Japan, and Morinaga foundation for health and nutrition (to YH).

AUTHOR CONTRIBUTIONS

Research idea and study design: KH and YH; acquired data: TH, HI, KM, KI, SH, and DO; data analysis: TH, KT, SU, and GT; supervision: TM, KH, and MH; draft writing: TH, YH, and SU All authors interpreted the results, revised the draft, and approved the final version of the manuscript.

SUPPLEMENTARY MATERIAL

Supplementary File (PDF)

Table S1. The list of 53 genes that represent monogenic causes of human focal segmental glomerulosclerosis and/or steroid-resistant nephrotic syndrome.

Table S2. Variant frequencies of the *NUP93* variants in our case.

Figure S1. Renal NUP93 expression in patients with proteinuria. Human kidney sections were stained with anti-NUP93 antibody (green), anti-CD2AP-antibody (red), and 4′,6-diamidino-2-phenylindole (DAPI) (blue).

REFERENCES

1. Bose B, Cattran D. Glomerular diseases: FSGS. *Clin J Am Soc Nephrol*. 2014;9:626–632.
2. D'Agati VD, Kaskel FJ, Falk RJ. Focal segmental glomerulosclerosis. *N Engl J Med*. 2011;365:2398–2411.
3. Sethi S, Glassock RJ, Fervenza FC. Focal segmental glomerulosclerosis: towards a better understanding for the practicing nephrologist. *Nephrol Dial Transplant*. 2015;30:375–384.
4. Trautmann A, Lipska-Zietkiewicz BS, Schaefer F. Exploring the clinical and genetic spectrum of steroid resistant nephrotic syndrome: The PodoNet Registry. *Front Pediatr*. 2018;6:200.
5. Saleem MA. New developments in steroid-resistant nephrotic syndrome. *Pediatr Nephrol*. 2013;28:699–709.
6. De Vriese AS, Sethi S, Nath KA, et al. Differentiating primary, genetic, and secondary FSGS in adults: a clinicopathologic approach. *J Am Soc Nephrol*. 2018;29:759–774.
7. Harita Y. Application of next-generation sequencing technology to diagnosis and treatment of focal segmental glomerulosclerosis. *Clin Exp Nephrol*. 2018;22:491–500.
8. Fogo AB. Causes and pathogenesis of focal segmental glomerulosclerosis. *Nat Rev Nephrol*. 2015;11:76–87.
9. Jefferson JA, Shankland SJ. The pathogenesis of focal segmental glomerulosclerosis. *Adv Chronic Kidney Dis*. 2014;21:408–416.
10. Bierzynska A, Soderquest K, Koziell A. Genes and podocytes—new insights into mechanisms of podocytopathy. *Front Endocrinol*. 2014;5:226.
11. Preston R, Stuart HM, Lennon R. Genetic testing in steroid-resistant nephrotic syndrome:why, who, when and how? *Pediatr Nephrol*. 2019;34:195–210.
12. Bierzynska A, McCarthy HJ, Soderquest K, et al. Genomic and clinical profiling of a national nephrotic syndrome cohort advocates a precision medicine approach to disease management. *Kidney Int*. 2017;91:937–947.
13. Sadowski CE, Lovric S, Ashraf S, et al. A single-gene cause in 29.5% of cases of steroid-resistant nephrotic syndrome. *J Am Soc Nephrol*. 2015;26:1279–1289.
14. Warejko JK, Tan W, Daga A, et al. Whole exome sequencing of patients with steroid-resistant nephrotic syndrome. *Clin J Am Soc Nephrol*. 2018;13:53–62.
15. Beck M, Hurt E. The nuclear pore complex:understanding its function through structural insight. *Nat Rev Mol Cell Biol*. 2017;18:73–89.

16. Dickmanns A, Kehlenbach RH, Fahrenkrog B. Nuclear pore complexes and nucleocytoplasmic transport: from structure to function to disease. *Int Rev Cell Mol Biol*. 2015;320:171–233.
17. Nofrini V, Di Giacomo D, Mecucci C. Nucleoporin genes in human diseases. *Eur J Hum Genet*. 2016;24:1388–1395.
18. Kosinski J, Mosalaganti S, von Appen A, et al. Molecular architecture of the inner ring scaffold of the human nuclear pore complex. *Science*. 2016;352:363–365.
19. Raices M, D'Angelo MA. Nuclear pore complex composition: a new regulator of tissue-specific and developmental functions. *Nat Rev Mol Cell Biol*. 2012;13:687–699.
20. Cho AR, Yang KJ, Bae Y, et al. Tissue-specific expression and subcellular localization of ALADIN, the absence of which causes human triple A syndrome. *Exp Mol Med*. 2009;41:381–386.
21. Ori A, Banterle N, Iskar M, et al. Cell type-specific nuclear pores:a case in point for context-dependent stoichiometry of molecular machines. *Mol Syst Biol*. 2013;9:648.
22. Ibarra A, Hetzer MW. Nuclear pore proteins and the control of genome functions. *Genes Dev*. 2015;29:337–349.
23. Raices M, D'Angelo MA. Nuclear pore complexes and regulation of gene expression. *Curr Opin Cell Biol*. 2017;46:26–32.
24. Dauer WT, Worman HJ. The nuclear envelope as a signaling node in development and disease. *Dev cell*. 2009;17:626–638.
25. Braun DA, Sadowski CE, Kohl S, et al. Mutations in nuclear pore genes NUP93, NUP205 and XPO5 cause steroid-resistant nephrotic syndrome. *Nat Genet*. 2016;48:457–465.
26. Harita Y, Kurihara H, Kosako H, et al. Phosphorylation of nephrin triggers Ca2+ signaling by recruitment and activation of phospholipase C-{gamma}1. *J Biol Chem*. 2009;284:8951–8962.
27. Ogino D, Hashimoto T, Hattori M, et al. Analysis of the genes responsible for steroid-resistant nephrotic syndrome and/or focal segmental glomerulosclerosis in Japanese patients by whole-exome sequencing analysis. *J Hum Genet*. 2016;61:137–141.
28. Li H, Durbin R. Fast and accurate short read alignment with Burrows-Wheeler transform. *Bioinformatics*. 2009;25:1754–1760.
29. McKenna A, Hanna M, Banks E, et al. The Genome Analysis Toolkit: a MapReduce framework for analyzing next-generation DNA sequencing data. *Genome Res*. 2010;20:1297–1303.
30. Abecasis GR, Auton A, Brooks LD, et al. An integrated map of genetic variation from 1,092 human genomes. *Nature*. 2012;491:56–65.
31. Lek M, Karczewski KJ, Minikel EV, et al. Analysis of protein-coding genetic variation in 60,706 humans. *Nature*. 2016;536:285–291.
32. Shih NY, Li J, Karpitskii V, et al. Congenital nephrotic syndrome in mice lacking CD2-associated protein. *Science*. 1999;286:312–315.
33. Udagawa T, Harita Y, Miura K, et al. Amnionless-mediated glycosylation is crucial for cell surface targeting of cubilin in renal and intestinal cells. *Sci Rep*. 2018;8:2351.
34. Nagasaki M, Yasuda J, Katsuoka F, et al. Rare variant discovery by deep whole-genome sequencing of 1,070 Japanese individuals. *Nat Commun*. 2015;6:8018.
35. Biasini M, Bienert S, Waterhouse A, et al. SWISS-MODEL: modelling protein tertiary and quaternary structure using evolutionary information. *Nucleic Acids Res*. 2014;42:W252–W258.
36. Waterhouse A, Bertoni M, Bienert S, et al. SWISS-MODEL: homology modelling of protein structures and complexes. *Nucleic Acids Res*. 2018;46:W296–W303.
37. Bezdicka M, Stolbova S, Seeman T, et al. Genetic diagnosis of steroid-resistant nephrotic syndrome in a longitudinal collection of Czech and Slovak patients: a high proportion of causative variants in NUP93. *Pediatr Nephrol*. 2018;33:1347–1363.
38. Galy V, Mattaj IW, Askjaer P. *Caenorhabditis elegans* nucleoporins Nup93 and Nup205 determine the limit of nuclear pore complex size exclusion in vivo. *Mol Biol Cell*. 2003;14:5104–5115.
39. Del Viso F, Huang F, Myers J, et al. Congenital heart disease genetics uncovers context-dependent organization and function of nucleoporins at cilia. *Dev Cell*. 2016;38:478–492.